Distances of Stars by mean of the Phase-lag Method

Sandra Etoka[1,2], Dieter Engels[2], Eric Gérard[3] and Anita M. S. Richards[1]

[1]Jodrell Bank Centre for Astrophysics, University of Manchester, UK
email: `Sandra.Etoka@googlemail.com`

[2]Hamburger Sternwarte, Universität Hamburg, Germany

[3]GEPI, Observatoire de Paris-Meudon, France

Abstract. Variable OH/IR stars are Asymptotic Giant Branch (AGB) stars with an optically thick circumstellar envelope that emit strong OH 1612 MHz emission. They are commonly observed throughout the Galaxy but also in the LMC and SMC. Hence, the precise inference of the distances of these stars will ultimately result in better constraints on their mass range in different metallicity environments. Through a multi-year long-term monitoring program at the Nancay Radio telescope (NRT) and a complementary high-sensitivity mapping campaign at the eMERLIN and JVLA to measure precisely the angular diameter of the envelopes, we have been re-exploring distance determination through the phase-lag method for a sample of stars, in order to refine the poorly-constrained distances of some and infer the currently unknown distances of others. We present here an update of this project.

Keywords. masers, stars: late-type, stars: variables: OH/IR, stars: distances

1. Introduction

Evolved stars at the tip of the AGB for low- and intermediary-mass stars experience heavy mass loss surrounding the star with a circumstellar envelope (CSE), which ultimately become opaque to visible light. These enshrouded OH/IR stars commonly exhibit strong periodic (ranging typically from 1 to 6 yr) ground-state OH maser emission in the 1612-MHz transition. Over 2000 OH masers of stellar origin are currently known in the Milky Way (Engels & Bunzel, 2015) and it is anticipated that the SKA will detect thousands of OH maser sources of stellar origin in the anti-solar Galactic hemisphere and Local Group of galaxies (Etoka *et al.* 2015). This makes OH/IR stars potentially valuable objects for a wide range of studies in our Galaxy but also for stellar-evolution metallicity-related studies.

Because OH/IR stars are optically thick, their distances cannot be inferred using optical parallaxes. The period-luminosity relation found towards Miras (Whitelock, Feast & Catchpole 1991) breaks down for P> 450 days. Kinematic distances can be very imprecise due to peculiar motions (Reid *et al.* 2009). As it has been extensively demonstrated in this symposium, maser emission at high(er) frequency from e.g. water and methanol species is successfully used to infer distances via parallax measurements towards distant Galactic star forming regions. The use of ground-state OH maser to infer distances of AGB stars via parallax measurements has also been successfully done but only for objects relatively nearby (i.e., $\leqslant$2 kpc; Vlemmings & van Langevelde 2007; Orosz *et al.* 2017). Another alternative to distance determination for more distant evolved stars is the use of the "phase-lag" method.

2. Method and Observations

The determination of the distance of an OH/IR star via the phase-lag method relies on the measurement of the linear and angular diameter of its OH-maser CSE which are both obtained independently. OH/IR stars typically exhibit a double-peaked spectral profile where the blueshifted peak ("blue" peak here after) emanates from the front cap of the CSE and the redshifted peak ("red" peak here after) emanates from the back cap of the CSE while the faint interpeak emission emanates from the outer part of the CSE. We measure the phase lag (τ_0) of a source with no external fitting function, using simply the shape of the light curve, by scaling and shifting the integrated-flux light curves of the blue peak F_b with respect to the red one F_r, minimizing the function $\Delta F = F_r(t) - a \cdot F_b(t - \tau_0) + c$ (where a and c are constants for the amplitude and mean flux) leading to the measurement of the linear diameter of the OH shell of the star. The angular diameter is obtained from interferometric mapping.

Schultz, Sherwood & Winnberg (1978) performed the first phase-lag measurements, and in the 1980's, Herman & Habing (1985) and van Langevelde, van der Heiden & van Schooneveld (1990) explored this method to retrieve distances from OH/IR stars, but there are discrepancies in the phase-lag measurement of a good fraction of the sources in common in these 2 works. In an attempt to constrain the distance uncertainties achievable with this method we are re-exploring it. Our sample consists of 20 OH/IR stars that we have been monitoring with the Nançay Radio Telescope (NRT) in order to measure their phase-lags. About half of the sample is composed of sources for which phase-lags were determined in the 1980's, the ones for which both works are in agreement serving as benchmark objects while for the objects with clear discrepancy the aim being re-determination of their phase-lag. The rest of the sample consists of objects with no recorded phase-lag measurements. About half of the sources of the sample have been previously imaged but the interferometric observations were taken at a random time and/or with poor sensitivity. We are currently in a process of imaging all the sources in the sample with either eMERLIN or JVLA around the OH maxima of each source, as predicted from the NRT light curves, in order to improve the angular diameter determination by detecting the faint interpeak signal and better constrain the shell (a)symmetries.

Past reports of the method and status of the project were presented in Engels *et al.* (2012, 2015) while a detailed description of the applicability of the method in measuring distances for objects beyond the solar vicinity can be found in Etoka *et al.* (2014). In the next section an update and discussion based on the results obtained so far is presented.

3. Discussion

Table 1 presents the summary of the results obtained so far. The first half of the table gives the range of periods, phase-lags and linear diameters inferred from the NRT monitoring from all the sources of the sample. The second half of the table gives the range of angular diameters and inferred phase-lag distances. The phase-lags measured account for linear shell diameter of $\sim$1700 to $\sim$19000 AU. Generally, the diameter is larger for longer-period objects. Distances ranges from 0.5 to 10.6 kpc. But, it has to be noted, that at the time of writing, although 70% of the sources of the sample have a measured angular diameters, 60% are from the literature including these 2 extremas.

Figure 1 presents the NRT monitoring and interferometric mapping for OH 83.4-0.9 and OH 16.1-0.3, two objects of the sample for which there was no previous imaging. We mapped both objects around their OH maximum with eMERLIN and the JVLA

Table 1. Summary of the periods, phase-lags, linear & angular diameters and distances inferred for the entire sample

		min.	max.
P^a	[yrs]:	1.16	6.05
$\tau_0{}^a$	[days]:	< 10	110
$2\,R_{OH}{}^a$	[10^3 AU]:	< 1.7	19
ϕ	["]:	0.8^b	8.0^b
D	[kpc]:	0.5^b	10.6^b

Table 2. Results for OH 83.4-0.9 & OH 16.1-0.3

Object	P [yrs]	τ_0 [days]	$2\,R_{OH}$ [10^3 AU]	ϕ ["]	D [kpc]
OH 83.4-0.9	4.11	30	5.2	∼1.8	∼3.0
OH 16.1-0.3	6.03	110	19.0	∼3.5	∼5.5

a: All the periods, phase lags and corresponding linear diameters are inferred from our NRT monitoring. The status of which can be followed here: `http://www.hs.uni-hamburg.de/nrt-monitoring`
b: from the literature
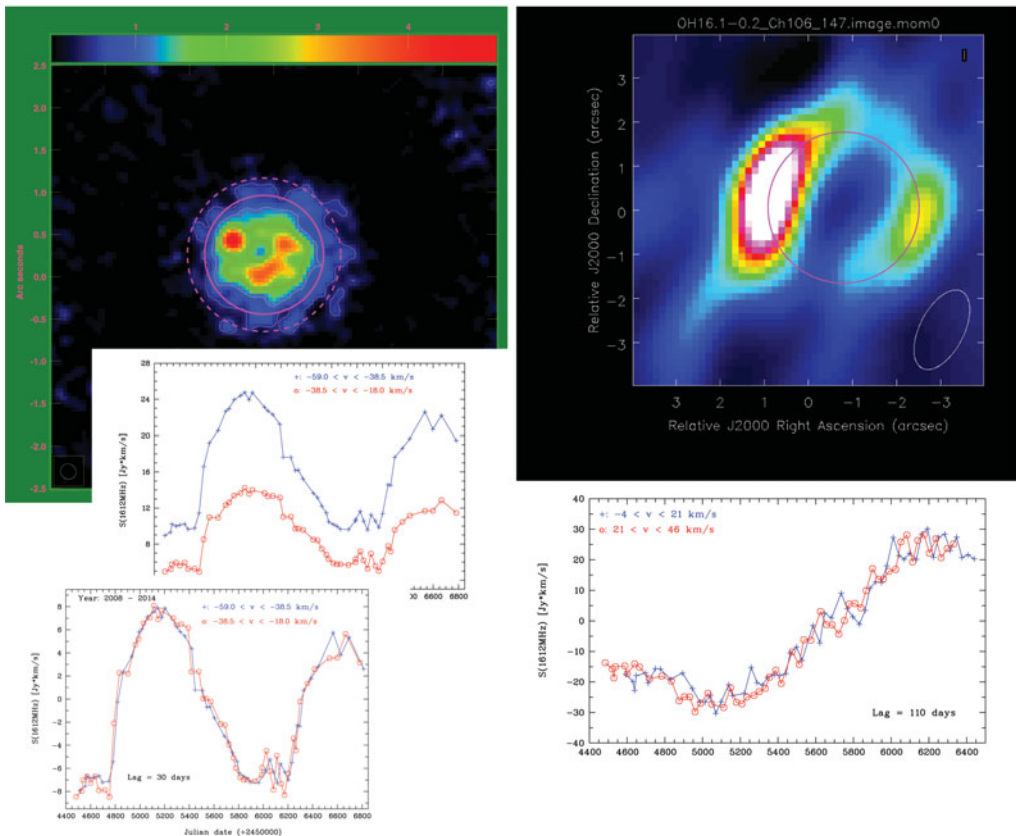
Figure 1. *Left main-panel:* eMERLIN map of the integrated emission over the inner part of the spectrum of OH 83.4-0.9 covering the velocity range $[-55;-23]$ km s^{-1}. The magenta full and dotted circles delineate the outer part of the shell. *main-panel insert:* spectrum. *middle:* "raw" blue-peak and red-peak light curves of OH 83.4-0.9 obtained from the NRT monitoring over a period of 7 years. *bottom:* scaled and shifted light curves for phase-lag determination. *Right main-panel:* JVLA map of the integrated emission over the red inner part of the spectrum of OH 16.1-0.3 covering the velocity range $[+27;+37]$ km s^{-1}. The magenta circle presents the best fit of the projected diameter of the shell. *main-panel insert:* Spectrum. *bottom:* scaled and shifted light curves for phase-lag determination.

respectively, which allowed us to retrieve a substantial amount of the faint interpeak emission. For both objects, the channel maps obtained are in agreement with the shells

being spherically-thin in uniform radial expansion. As an illustration of the phase-lag determination method explained in Section 2, the left middle- and bottom-panels show the "raw" blue-peak and red-peak light curves of OH 83.4-0.9 and the scaled and shifted light curves leading to the phase-lag measurement. The period, phase lags and corresponding linear & angular diameters measured and subsequent inferred distances for these 2 objects are summarized in Table 2. For these 2 objects, we estimated the uncertainty of the linear diameter to be within 10%, while that of the angular diameter to be within 15%, leading to a distance determination uncertainty of less than 20%. On the other hand, the distance determinations given in Table 1 are still questionable as strongly dependent on the degree of exploration for the shell extent determination, i.e., faint tangential emission, which not only allow to better constrain the actual extent of the shell, but also its actual geometry, as in particular, a strong deviation from a spherically thin shell in uniform radial expansion can lead to distance uncertainty greater than 20% (Etoka & Diamond, 2010).

4. Closing Notes

The main contribution to the early phase-lag inconsistencies could be due to: incomplete coverage of lightcurves; inhomogeneous sampling; use of analytical functions to fit the lightcurves. Phase-lag distances can be determined with an uncertainty of less than 20%, provided that a good constraint on both the linear and angular diameter determinations can be achieved. The main factors for doing so are the following:

• the shape of the light curves must be well defined. This can be obtained with high cadence monitoring observations (i.e., typically with 0.03 P);

• the light curves cover more than one period;

• the faint tangential emission tracing the actual full extent of the shell can be imaged via high-sensitivity interferometric observations better retrieved around the maximum of the OH cycle;

• significant shell asymmetries can be excluded or modelled.

References

Engels, D. & Bunzel, F. 2015 *A&A*, 582A, 68
Engels, D., Etoka, S., Gérard, E., & Richards, A. M. S. 2015, *ASPC*, 497, 473
Engels, D., Gérard, E., & Hallet, N., 2012, *IAUS* 287, 254
Etoka, S., Engels, D., Imai, H. *et al.* 2015, *Proc. Science*, (AASKA14), 125
Etoka, S., Engels, D., Gérard, E., & Richards A. M. S. 2014, *evn conf*, 59
Etoka, S. & Diamond, P. D. 2010, *MNRAS*, 406, 2218
Herman, J. & Habing, H. J. 1985, *A&AS*, 59, 523
Orosz, G., Imai, H., Dodson, R. *et al.* 2017, *AJ*, 153, 119
Reid, M. J., Menten, K. M., Zheng, X. W. *et al.* 2009, *ApJ*, 700, 137
Schultz, G. V., Sherwood, W. A., & Winnberg, A. 1978, *A&A*, 63L, 5
van Langevelde, H. J., van der Heiden, R., & van Schooneveld, C. 1990, *A&A*, 239, 193
Vlemmings, W. H. T.. & van Langevelde, H. J. 2007, *A&A*, 472, 547
Whitelock, P., Feast, M., & Catchpole, R. 1991, *MNRAS*, 248, 276